

Layer 2-5 Mechanical Design

The outer four layers of the tracker consist of 168 staves, 84 in each sub-barrel. Each stave contains four silicon modules, two axial and two small angle stereo. The stave provides active cooling to remove the heat generated by the readout electronics and the sensors, maintains the planarity of the silicon sensors, and provides for the accurate alignment of the sensor planes in space.

Readout configuration

The azimuthal multiplicity of each sensor layer must be divisible by 6 in order to fit in the existing silicon track trigger. Although not a hard constraint, we felt it very desirable to limit the number of sensor and hybrid types, our goal being only one sensor type for all four outer layers. This leads to ϕ segmentation of 12, 18, 24 and 30 in layers 2, 3, 4 and 5, respectively. Given the radii of these layers (≈ 50 -160mm) the necessary sensor active width is determined to be 32-38mm. We wish to produce two sensors per 6" silicon wafer, so the length of the sensors is limited to ~ 110 mm. To obtain the desired η coverage, layers 2-5 should have 600mm of sensor coverage (each side of $z=0$). This leads to a natural choice of 100mm for the sensor length.

The readout cable plant is limited to about 912 by the existing electronics. Of these, 216 are reserved for the inner two layers of the tracker. Dead time considerations limit the total number of SVX channels that can be accommodated on one readout cable; this limit is 10 chips for layers 2-5. The available cable plant cannot accommodate fine pitch (50-60 μm) readout with fine (100 mm) z-segmentation. Simulations of resolutions, pattern recognition and occupancy found a substantial preference for finer pitch over finer z segmentation. In addition, finer pitch also allows for direct wire bonding from the SVX chips to the sensors. We have chosen a sensor design with 639-channels at 60 μm pitch, for an active width of 38.4 mm.

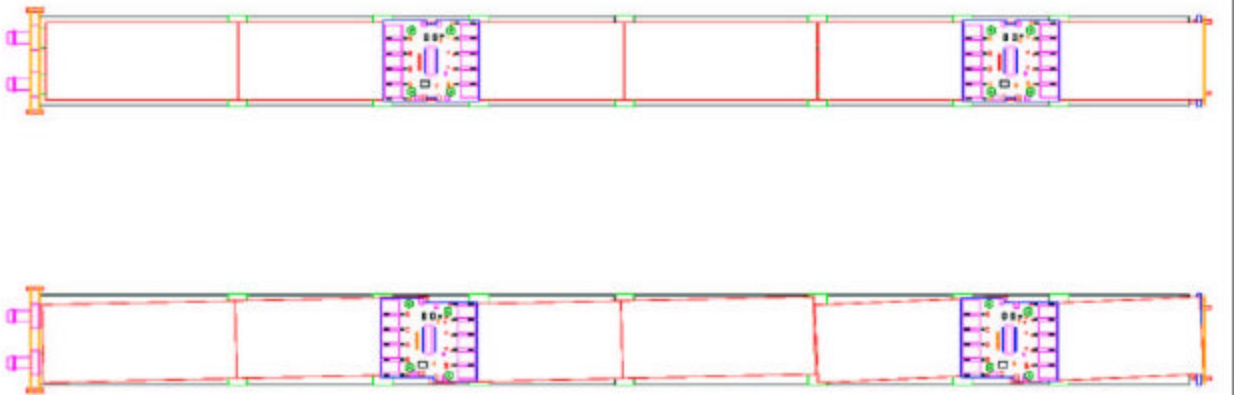


Figure 1: Readout configuration for outer layer staves. The axial modules are shown above and the stereo modules below.

The outer layers (layers 2-5) contain staves six sensors long (Figure 1). The hybrid-sensor modules closest to $z=0$ within a stave are 200 mm long and have two 100 mm readout segments. Those further from $z = 0$ are 400 mm long and have two 200 mm readout segments. To form the 200 mm readout segments, two 100 mm sensors are glued

end-to-end and electrically coupled with wirebonds on the top surface and a bias connection between the back planes.

Silicon modules

The outer layer silicon modules consist of two or four silicon sensors, each 100 mm in length by 40.34 mm in width, joined together with a single readout hybrid. The readout hybrid is double-ended, meaning that the hybrid straddles two sensors with separate SVX chips reading out the signals from each end. There are four types of modules labeled by the length in centimeters of the sensor segment read out and whether their sensors are aligned axially or with a stereo angle. The same sensors are used in all four of the module types. There are two hybrid types, one for the axial modules and one for the stereo modules. The two axial modules differ only in the number of sensors used, while the two stereo module types use different stereo angles depending on the lengths of the readout segments; 1.24 degrees for 200mm readout, 2.48 degrees for 100mm readout. While the larger stereo angle would be preferred throughout the device, tight geometrical constraints limit the width of the staves, and hence the maximum allowable stereo angle as a function of readout length.



Figure 2: Module assemblies. Top: A 20-20 axial module. Bottom: A 20-20 stereo module.

Each hybrid has 10 SVX chips, 5 at each end of their 50mm length. Each SVX chip generates 0.3-0.5W of heat, with 50% of that heat load concentrated in narrow regions near the two ends of the chip. For design purposes we have assumed a 0.5W load per chip. A connector located at the center of the hybrid provides the power, control signals for the chips and the high voltage for the sensor bias. A bias line wraps around the edge of the sensor to provide a connection directly to the back plane of the sensor. Ground connections also wrap around the edge of the sensor-hybrid modules to tie the conductive support structure to the local hybrid ground in order to minimize ground current and pickup effects.

The techniques for assembly of sensor modules are similar to those used in the past by many groups, including DØ. Sensors are manually aligned with optical feedback from a camera mounted on a coordinate measurement machine (CMM). Once aligned, the

sensors are glued to one another, directly or via a connecting substrate. Reasonable expectations for this alignment are a few microns. The hybrid, previously assembled, burned-in and tested, is glued directly to the silicon sensors. Wire bonding is then done between the hybrid and the sensors, and from sensor to sensor for the modules with 200mm readout segments. The sensor pitch has been chosen so that the hybrid to sensor bonding can be done directly from the SVX chips to silicon sensors without a pitch adapter. The total numbers of wire bonds required for layers 2-5 are 430K sensor-to-sensor plus 860K hybrid-to-sensor, for a total of 1290K bonds. For the longer modules, the sensor-to-sensor wire bonding can be done either before or after the hybrid is mounted. Sensor alignment and sensor-to-sensor wire bonding can proceed prior to hybrid delivery, should that become a production constraint.

Prior to assembly into staves the completed module will undergo electrical testing, additional burn-in and in some cases laser scanning (described elsewhere in this document).

Stave assemblies

The outer four layers of the silicon tracker are constructed as 168 staves, approximately 46mm wide by 8.9mm tall by 610mm in length (Figure 3). Each stave is independently mounted to a set of bulkheads, described previously. The stave structures consist of a core with silicon mounted to both surfaces and two external C-channels that stiffen the structure. The core structure has an integrated cooling circuit to remove the heat generated by both the hybrid electronics and the silicon sensors. The core also provides the precise reference features for aligning and mounting sensor modules to the core and the completed stave to the bulkheads. Finally, the core maintains the flatness of the silicon sensors. The external C-channels provide the necessary bending and torsional stiffness to the stave.

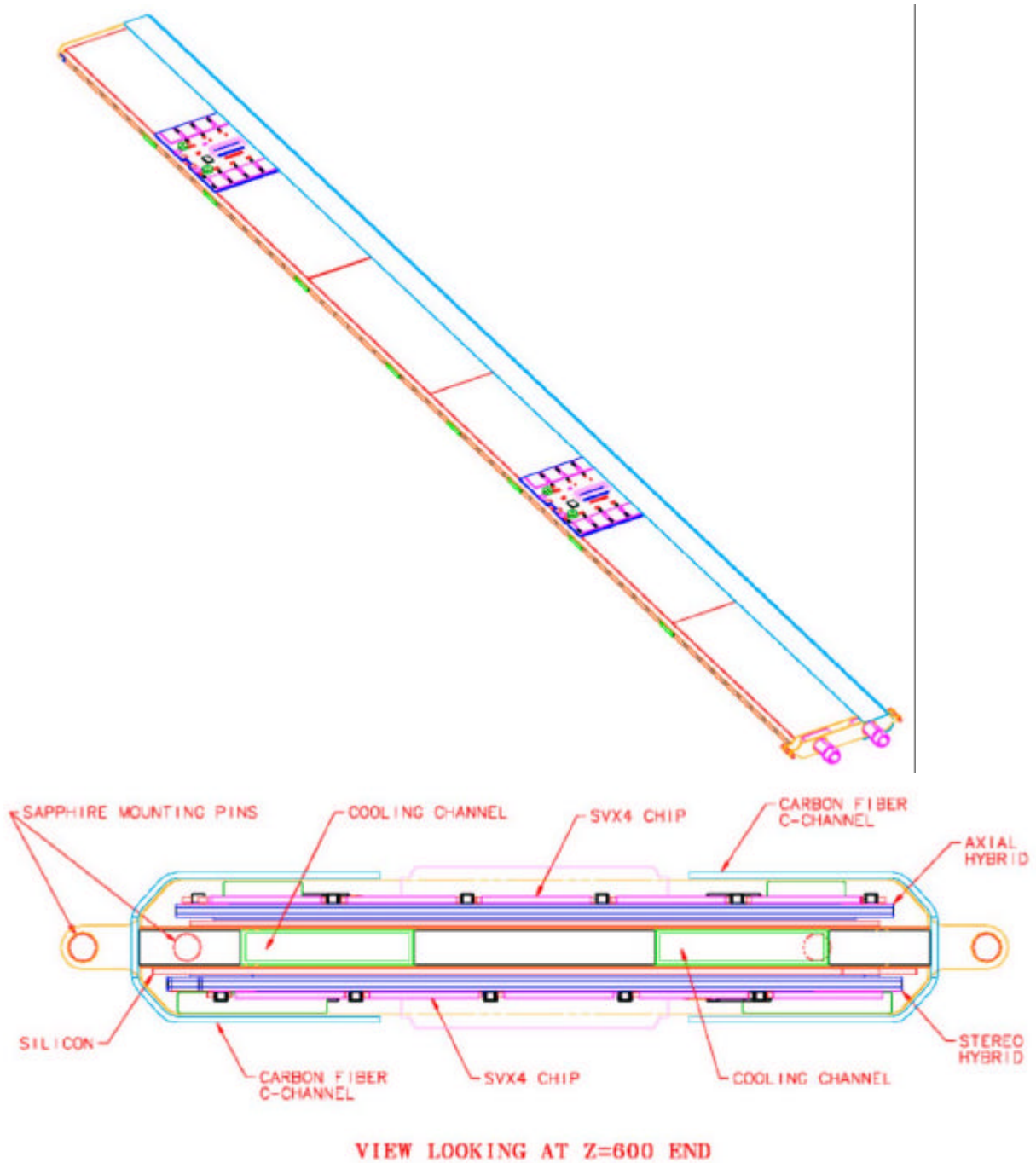


Figure 3: Stave assembly drawings. The upper drawing shows a isometric view of the stave with one of the C-channels removed. The lower plot is an end view of a complete stave assembly.

The core structure is about 2mm tall. The main element is the cooling tube. The tube is made from high strength carbon fiber (IM7 or similar) with a cyanate ester resin (Bryte EX-1515 or similar) that features very low moisture absorption. The cooling passage is

2mm tall by 10mm wide (outside) with a 200-250 micron wall thickness. The tube is a U-shape, turning around near $Z=0$. The mechanical structure is built up from this tube using “outriggers” made of similar tube to carry the silicon module load out to the C-channels. The remaining space will likely be filled with Rohacell foam to provide a uniform mounting surface for the sensors. The core structure will be laminated with 50 micron Kapton MT, a polyimide loaded with alumina for better thermal conductivity, to provide an electrically insulating layer between the back plane of the sensors, at 300V, and the tube, which will be grounded. The fluid dynamics, thermal performance and mechanical performance of this structure are described below. Precision mounting and alignment features - ruby and sapphire rods and spheres - are an integral part of the core structure. Once assembled, the core structure can be leak checked and inspected for dimensional tolerances prior to population with silicon modules.

The silicon modules are bonded directly to the stave core. One side of the core is populated with axial sensor modules while the other is populated with small angle stereo modules. The mounting and reference features on the stave core are accessible from both sides of the stave so that they can be used to establish the reference system on a CMM for alignment of the silicon modules to the stave core. Past experience is that module-to-module alignment can be done at the sub- 5μ level.

Carbon fiber C-channel structures mount to the core on each side with cross-members at several locations along the length of the stave. These structures provide most of the stiffness of the completed stave, provide a surface for the readout cables to attach to as they run to the end of the stave, and help to protect the sensors and hybrids from damage during further processing steps.

Stave mass and radiation length

The stave mass and radiation length have been estimated. The stave weight per unit length is 2.38g/cm. The radiation length (Table 1), averaged over the silicon area, is 2.53% X_0 per layer. The breakdown of the material is 0.68% X_0 sensors, 0.55% X_0 hybrids, 0.56% X_0 readout cables, 0.31% X_0 coolant and tube, and 0.43% X_0 for the stave structure and adhesives. The equivalent of 1.5 readout cables are included in this estimate; the first cable begins at $Z=100$ mm and the second at $Z=400$ mm. A track passing at normal incidence through the hybrids sees roughly 5.3% X_0 per layer. Near $Z=0$, where there are no cables or hybrids, the radiation length is only 1.4% X_0 per layer.

Table 1 - Breakdown of stave radiation length by material. The table below is for the layer 4-5 staves.

Item	Material	X0 (cm)	L (mm)	W (mm)	t (mm)	%X0 (local)	%X0 (avg.)	Fraction
Silicon Sensor	Si	9.4	600.0	40.3	0.640	0.681	0.681	26.9%
SVX4 chips (5x2)	Si	9.4	36.0	32.0	0.720	0.766	0.036	
Epoxy (loaded, 50 microns)	Loaded epoxy	10.0	36.0	32.0	0.100	0.100	0.005	
BeO substrate	BeO	13.3	100.0	38.4	0.760	0.571	0.091	
Dielectric layers	glass	12.7	100.0	38.4	0.720	0.567	0.090	
Metal Layers	Au	0.3	100.0	38.4	0.029	0.960	0.152	
Surface Mount comps.	High Z	1.0	37.6	11.0	0.500	5.000	0.085	
Solder	Pb/Sn	0.9	26.2	38.4	0.200	2.222	0.092	21.8%
CF tube (2 x 10mm x 2mm)	CF	25.0	600.0	20.0	0.575	0.230	0.114	
Coolant	40% EG	35.8	600.0	19.0	1.500	0.419	0.197	12.3%
Skins (Kapton MT)	Kapton	28.4	600.0	46.2	0.100	0.035	0.040	
Rohacell 51 foam spacer	Rohacell 51	806.0	600.0	26.2	1.778	0.022	0.014	
Pins	Sapphire	7.3	18.0	1.6	1.245	1.705	0.002	
Pin holders (G-10 and CF)	G-10	19.4	18.0	16.0	1.900	0.979	0.012	
Epoxy (structural)	Epoxy	35.0	600.0	46.2	0.150	0.043	0.049	4.6%
C-channels	CF	25.0	600.0	36.0	0.760	0.304	0.271	
Epoxy (structural)	Epoxy	35.0	600.0	3.0	0.500	0.143	0.011	12.0%
Readout cables Kapton	Kapton	28.4	600.0	14.9	0.467	0.164	0.061	
Readout cable copper	Cu	1.4	600.0	11.9	0.235	1.680	0.496	22.0%
Total							2.531	100.0%

Stave mechanical connection

The staves are mounted to a pair of bulkheads, located at $Z=0$ and $Z=600$ mm, that are coupled to each other by carbon fiber cylinders. The carbon fiber cylinders have a coefficient of thermal expansion (CTE) very near zero, while the staves are expected to shrink by roughly 6μ between assembly at room temperature and operation with -14 C coolant (see Figure 5 in the section on stave thermal performance). In addition there may be some relative motion of the bulkheads, particularly longitudinally, during transportation and installation of the device. In the transverse direction the spacing between the mount points is ~ 50 mm so the differential contraction of the stave and carbon fiber bulkheads is only expected to be $2-3\mu$. This is negligible and need not be considered in the mount design. Were the bulkheads fabricated in beryllium rather than carbon fiber this differential contraction would be 15μ and the mounts would need to be redesigned to allow for this.

In order to allow for longitudinal motion we intend to use mounts consisting of sapphire rods inserted into ruby orifices. These parts are commercially available with a tolerance range of $\pm 5\mu$ on the fit. The stave will have two pins located at the outer end that engage the outer bulkhead at either side of the stave along the stave mid-plane, and similarly at the $Z=0$ end two pins emerge from between the sensors to engage the $Z=0$ membrane. A longitudinal constraint will fix the $Z=600$ mm end of the stave to the outer bulkhead, allowing the stave to retract from the $Z=0$ membrane during cool-down. A four-point

mount is necessary since the staves do not have large torsional stiffness ($\theta/\tau=1\text{mrad}/120\text{g}\cdot\text{mm}$) compared to their mass (140g) and width (40mm).

Alignment precision and stave mounts

The alignment requirements for the sensors are determined by the requirements of the impact parameter trigger. The trigger does not have the stereo sensor information so any misalignment of the axial sensors to the beam axis results in a degradation of the $r\text{-}\phi$ resolution at the trigger level. The intrinsic device resolution is $\approx 8\mu$.

The roll angle, i.e. rotation around an axis parallel to the beam line, does not affect trigger resolution, provided that it is known from survey. For a rotation in the plane of the sensors (yaw), the desired alignment tolerance is $<10\mu$ over a readout segment, or an angle of $<50\mu\text{rad}$. This results in an r.m.s. alignment tolerance of $\pm 30\mu$ over the full stave length. The pitch angle affects strips at the edges of the sensors, but not at the center. For a radial deviation dR at an angle ϕ from the center of the sensor, the transverse measurement error dX is given by $dX=dR\tan\phi$. The worst case is at the edges of the sensors where $\tan\phi=0.27(0.11)$ in layer 2(5). This implies a radial positioning tolerance of $\pm 110(285)\mu$ over the length of a stave in layer 2(5). If the sensors are not held flat within the stave the effect is identical to that of the pitch angle. Here the length scale is 100mm, so the tolerance on the sensor flatness is of order 20μ . It is difficult to anticipate the degree of warping which the production sensors will have due to stresses induced in manufacturing. Very flat vacuum fixtures will be used to hold the sensors flat during bonding to the core. The 2mm tall core structure with sensors on both sides provides a significant moment of inertia to constrain the sensors flat.

The tolerances on the pins and orifices intended for mounting the staves are sufficiently tight to permit a mounting system without adjustment, provided the orifices can be located in the bulkheads with high precision. This is considered to be feasible.

Layer 2-5 stave thermal performance

The mechanical and thermal characteristics of the staves have been evaluated both analytically and using finite element analysis (FEA). The radiation environment of Run IIb affects both the depletion voltage and the leakage current (noise) of the silicon sensors. The former depends on the magnitude of the reverse annealing term, which saturates for temperatures below 0C and is fairly insignificant up to temperatures of +10C. Here the relevant temperature is the peak temperature on the sensors. The leakage current for a strip, and hence the associated noise, depends on the integrated current along the strip, and hence is a function of the average temperature, with appropriate weighting, along the strip. We have used the FEA temperature profiles to calculate the expected strip currents and then used this to extract an equivalent temperature, corresponding to the uniform temperature that would produce the same leakage current. Our design goal is $<15\%$ degradation in signal to noise ratio, with a minimum S/N of 10 at 20fb^{-1} . The result is that the equivalent temperature should be kept below 0C in layer 2 and below +5C in layers 3-5.

The stave cooling channel will operate below atmospheric pressure, hence the pressure drop is limited to $\approx 3\text{psi}$. The total stave heat load is dominated by the hybrids that generate up to 20W, while the sensors are not expected to contribute more than 3W in layer 2 after 30fb^{-1} of exposure. The expected operating point for the stave is a flow rate

of 0.175lpm resulting in a pressure drop of 2.6psi from inlet to outlet with a bulk temperature rise of 1.9C. The tube wall will operate roughly 7C above the bulk temperature locally under the hybrids.

Figure 4 shows the result of a finite element analysis (FEA) of the stave structure. This model assumes a heat transfer coefficient of $835\text{W/m}^2\text{K}$, as expected for the design flow, and an inlet fluid temperature of -14C . The maximum temperature on the structure is -1.0C on the hybrid, while the maximum temperature on the sensor is -4.3C .

Experimental studies are underway to confirm the FEA results. Figure 5 shows the thermal distortions expected in the silicon sensors, perpendicular to the plane of the sensor and longitudinally. The thermal distortions are less than 10μ .

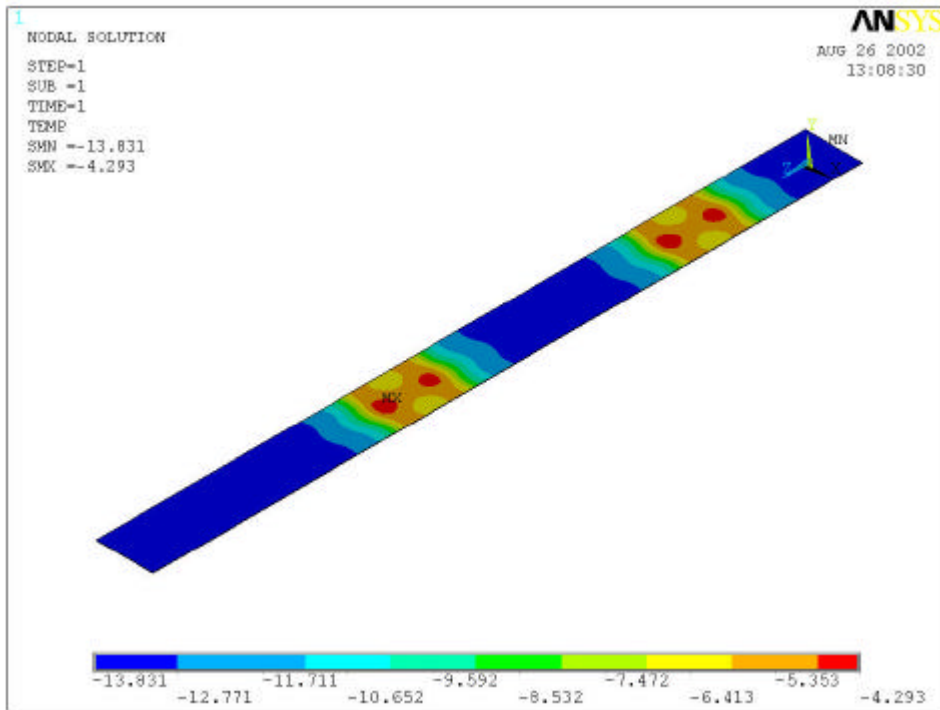
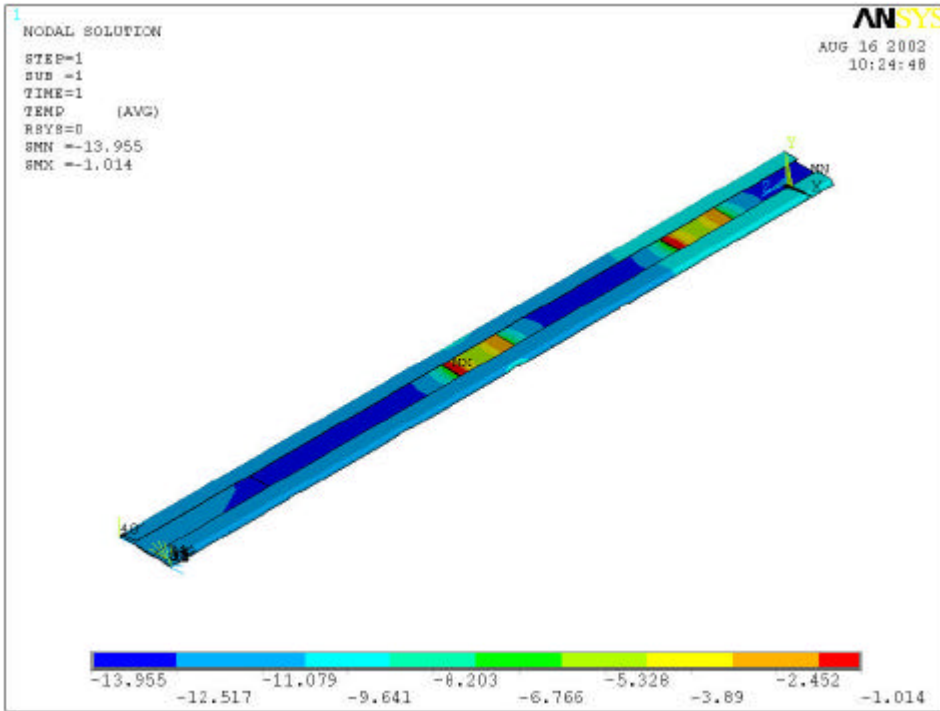


Figure 4: FEA results for the stave temperature profile. Coolant is assumed at -14C with a heat transfer coefficient of 835 W/m²K. The upper plot shows the full stave structure, with the hottest region on the SVX chips, while the lower plot shows only the silicon sensor temperature profile.

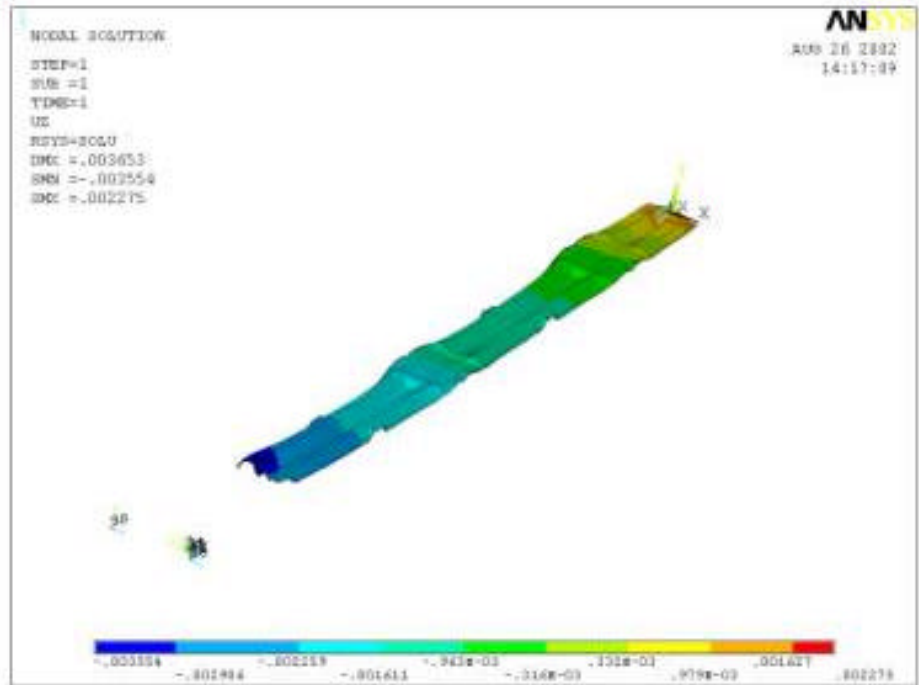
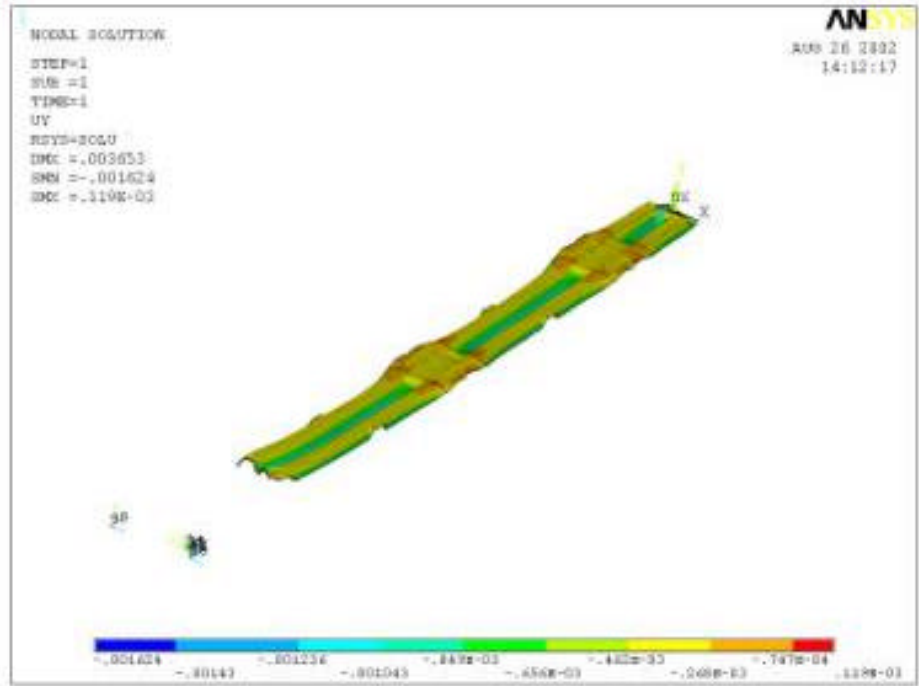


Figure 5: FEA results for the stave thermal distortion. Coolant temperature is -14°C . Dimensions shown are in mm. The upper plot shows the displacement perpendicular to the sensor planes, the lower plot the displacement along the axis of the stave. Only the silicon is shown in the figures. Note that the object shown is $\frac{1}{2}$ width, where a symmetry boundary condition is used along the centerline (far edge) of the stave.

Layer 2-5 stave mechanical performance

Mechanical performance of the stave has been evaluated using both analytical and FEA calculations, with good agreement between these results. The expected deflection of the staves is under 60μ with static gravitational loading (Figure 6). While somewhat larger deflections may not adversely affect the detector resolution, they lead to stave natural frequencies that are approaching the 60Hz range and the possible reduction in stave mass is negligible compared to the mass of the sensors, electronics and cables. In addition, reduced deflection allows for tighter installation and assembly clearances and easier handling during fabrication and installation of the staves into the barrel assemblies.

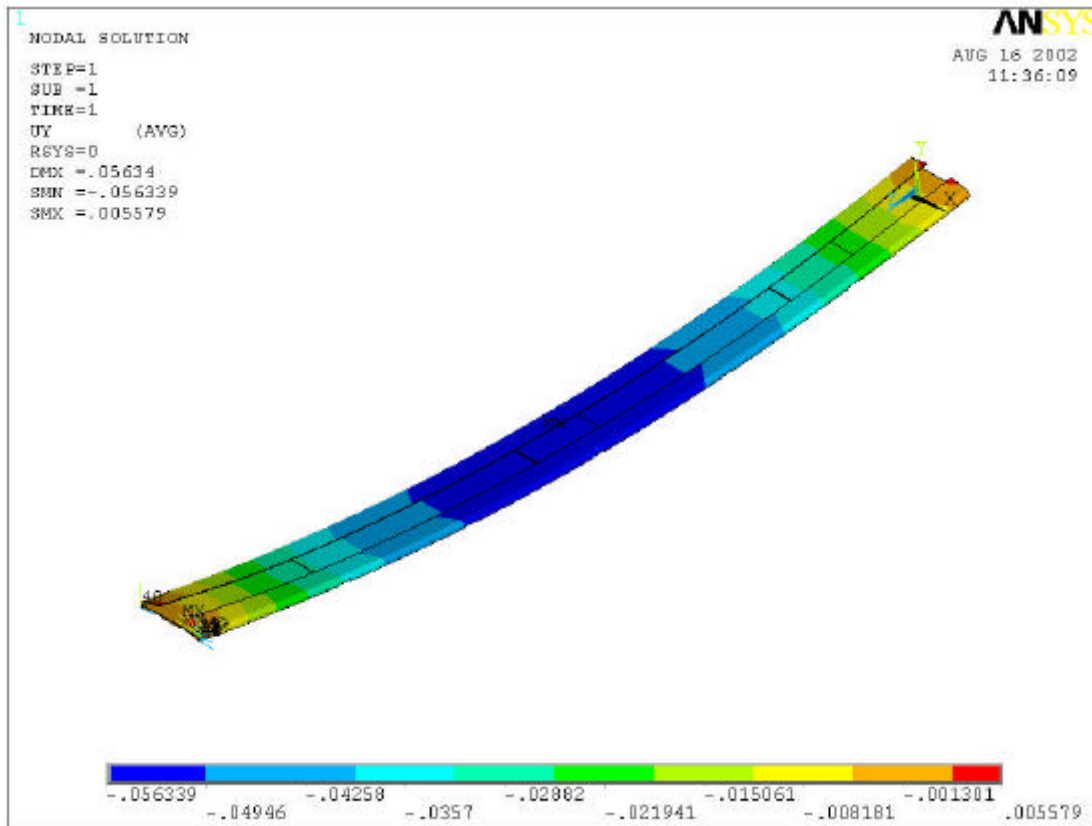


Figure 6: Stave deflection results for gravitational loading.

We have looked at extreme load conditions, for example application of a 1 kg load at the center of the stave, to study the robustness of the design. We find that, while the deflections are quite large, the stress levels in the sensors and structural elements remain far from failure levels. These studies were primarily aimed at understanding the handling requirements during fabrication and assembly.

A critical issue for the sensor alignment precision is deflection of the staves from external loads, in particular loads induced through the cables and cooling lines. To induce a 100μ deflection at the center of the beam requires a moment of 35kg-mm (3.0in-lbs). This is well above what could be induced through the external connections to the staves.